Intra-decadal variability in the Ekman heat flux from scatterometer winds

O. T. Sato and P. S. Polito

Instituto Nacional de Pesquisas Espaciais (INPE), Divisão de Sensoriamento Remoto, São José dos Campos, SP, Brazil

W. Timothy Liu

Jet Propulsion Laboratory/Caltech, Pasadena, CA, USA

Received 21 January 2002; accepted 18 June 2002; published 7 September 2002.

[1] We examine evidences of low frequency variability in the Ekman heat flux due to changes in the global temperature and wind patterns. The 10-year long time series of high resolution surface wind vectors was provided by the European Remote Sensing Satellites 1 and 2. A linear regression of the zonally averaged Ekman heat flux shows a latitudinal trend for the period between 1992 and 1997. This trend indicates a decrease in the poleward Ekman heat flux of warmer waters from the tropics and a slight decrease in the equatorward flux in the high latitudes. This intra-decadal trend ended after the 1998 El Niño event. These variations are mostly due to changes in the wind stress field. The decrease in the poleward Ekman heat flux may have far reaching consequences involving the global heat balance. *INDEX TERMS:* 4215 Oceanography: General: Climate and interannual variability (3309); 4504 Oceanography: Physical: Air/sea interactions (0312); 1640 Global Change: Remote sensing; 4572 Oceanography: Physical: Upper ocean processes; 3339 Meteorology and Atmospheric Dynamics: Ocean/atmosphere interactions (0312, 4504). **Citation:** Sato, O. T., P. S. Polito, and W. T. Liu, Intra-decadal variability in the Ekman heat flux from scatterometer winds, *Geophys. Res. Lett.*, *29*(17), 1831, doi:10.1029/2002GL014775, 2002.

1. Introduction

[2] The focus of this study is on the wind-driven or Ekman component of the oceanic circulation. Ekman dynamics is associated with upper layer temperature changes and has a significant impact in the total oceanic heat flux. The wind stress over the surface generates mass and heat fluxes in the first ten to a hundred meters of the ocean, the Ekman layer. The mass flux in the Ekman layer is not significantly large compared to the rest of the water column. However, depending on the latitude the Ekman heat flux (EHF) is comparable to the total because of the high temperatures associated within the Ekman layer. *Kraus and Levitus* [1986] analysis of climatological data showed that about 50% of the heat flux in the tropical Atlantic and almost all in the tropical Pacific are dominated by the EHF. According to *Sato and Rossby* [2000] the phase of the annual cycle of the total heat flux estimated from 60 years of historical data at 36°N in the Atlantic is dominated by the EHF. Results from ocean circulation models also showed that the inter-annual variability in the total heat transport is dominated by Ekman fluctuations [*Dong and Sutton*, 2001].

[3] The estimation of the total global energy budget is an intrinsically complex problem because it relies on a precise determination of various heat flux sources. Most of the heat budget studies use climatological data to estimate the heat balance in the interface or direct measurements of the currents to estimate the ocean heat. Currently, except for the Ekman, none of the other components include temporal variations because the available data are either climatological or sparsely distributed.

[4] The EHF has been estimated in a global scale using wind stress from in situ climatological data [*Kraus and Levitus*, 1986; *Levitus*, 1987; *Adamec et al.*, 1993] and from satellite-derived winds [*Ghirardelli et al.*, 1995]. The EHF is also estimated for specific locations when combined with direct measurements of the meridional heat flux [*Sato and Rossby*, 2000; *Hall and Bryden*, 1982; *Bryden et al.*, 1991; *Macdonald and Wunsch*, 1996]. The European Remote Sensing Satellites 1 and 2 (ERS) scatterometer provided an unprecedented 10-year long time series of surface winds vectors over the globe. Before the advent of such a global wind-stress time series the estimation of the seasonal cycle in the EHF had a limited accuracy [*Böning and Herrmann*, 1994]. This continuous source of data enables us to investigate inter-annual to intra-decadal variability in the global EHF.

2. Theory and Methods

[5] The meridional component of the EHF is defined as:

$$EHF = -c_p \int_0^L \frac{\tau_x}{f}\left(\theta_e - \bar{\theta}\right) dx \qquad (1)$$

where c_p is the specific heat at constant pressure which is assumed constant and equal to $4.1 \times 10^3 J\, kg^{-1}\, K^{-1}$, τ_x the zonal component of the wind stress, f the Coriolis parameter, θ_e the potential temperature of the Ekman layer, and $\bar{\theta}$ the mean potential temperature of the water column. The EHF is given in PW (peta Watts, $1\ PW = 10^{15}\ W$).

[6] Heat flux only makes sense when estimated in a closed system where the mass is conserved [*Montgomery*, 1974]. Therefore, to properly express the heat flux through the Ekman layer at each latitude its volume transport should be balanced by an equal and opposite deeper flow. Results from a high-resolution model of the Atlantic showed that

Copyright 2002 by the American Geophysical Union.
0094-8276/02/2002GL014775$05.00

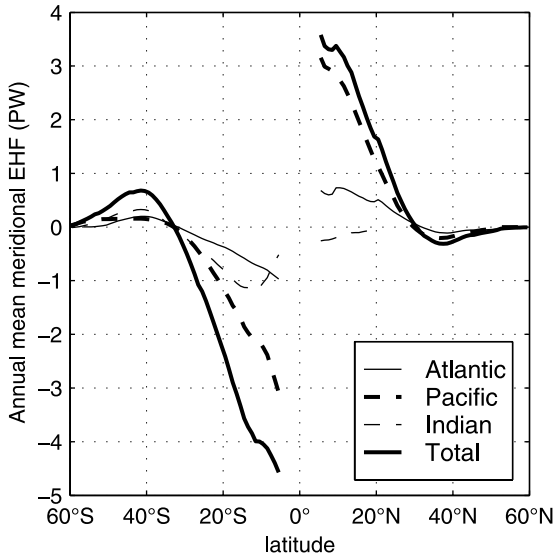

Figure 1. Annual mean of the Ekman heat flux (PW) for all ocean basins.

the return flow should extend to at least 3000 m in the extra-tropical region [*Böning and Herrmann*, 1994]. In this scenario, the temperature difference ($\theta_e - \bar{\theta}$) is a result of the conservation of mass. We used the World Ocean Atlas 1994 [*Levitus and Boyer*, 1994] to estimate the temperature of the compensating flow. The $\bar{\theta}$ is obtained through the use of the layer thickness as a set of weights to average the temperatures from 0 to 5000 m and generate one annual mean map with a $1^\circ \times 1^\circ$ resolution.

[7] Some studies assumed the sea surface temperature (SST) as a first approximation of the temperature of the Ekman layer [*Kraus and Levitus*, 1986; *Levitus*, 1987; *Adamec et al.*, 1993; *Ghirardelli et al.*, 1995]. Other studies used a weighted average temperature in the mixed layer [*Bryden and Hall*, 1980; *Rago and Rossby*, 1987]. In this study the temperature profiles in the Ekman layer incorporate contributions from high resolution maps of SST and climatological temperature profiles. The mean temperature (θ_e) was obtained by weight-averaging the constructed temperature profiles within the Ekman layer. This average uses the meridional component of a canonical Ekman spiral velocity profile as weights [*Sato and Rossby*, 2000]. Maps of SST came from the Reynolds data set from 1991 to 2001 [*Reynolds and Smith*, 1994] and were interpolated to a $1^\circ \times 1^\circ \times 10$ days grid. The subsurface temperature profiles were built from monthly mean climatological temperatures within 10 and 100 m from the World Ocean Atlas 1998.

[8] The zonal component of the wind stress (τ_x) is derived from bulk parameterization and flux equations based on the similarity theory [*Liu et al.*, 1979]. The wind stress estimates are calculated using the magnitude of the scatterometer wind, SST, and integrated water vapor. The water vapor data are obtained from the Special Sensor Microwave Imager (SSMI) satellite distributed in a daily basis since 1988. For the estimation of τ_x, all the data are sub-sampled (vapor) or interpolated (SST and wind) to maps of $1^\circ \times 1^\circ \times 10$ days.

[9] To investigate the inter-annual variability in the EHF we first need to examine the seasonal and basin-scale signals of τ_x. The wind stress is decomposed by a series of 2D finite impulse response filters [*Polito et al.*, 2000] as:

$$\tau_x = \bar{\tau} + \tau_l + \tau_r. \quad (2)$$

$\bar{\tau}$ is the long-term mean component. τ_l is the basin-wide and other large-scale non-propagating variability, mostly due to seasonal changes. τ_r is composed of propagating signals related to planetary waves, a variety of meso-scale eddy variability, and small-scale non-propagating signals. We are interested in examining only the mean ($\bar{\tau}$) and the non-propagating (τ_l) components as the propagating signals are related to higher frequencies.

3. Results and Analysis

[10] The annual mean meridional EHF estimated using scatterometer data as a function of latitude is poleward in the tropical Atlantic, Pacific, and South Indian oceans, Figure 1. The EHF is estimated outside the equatorial band from 5°S to 5°N. The magnitude of the annual mean of the zonally averaged EHF is lower than values obtained by climatological data [*Levitus*, 1987]. The mean is also slightly lower than values from SSMI derived winds [*Ghirardelli et al.*, 1995]. Mainly, the differences depend on the choice for the temperature of the Ekman layer and the source and method used to estimate the wind stress. The adoption of a velocity-weighted average instead of SST to represent the temperature of the Ekman layer decreases the EHF estimates. Tests (not shown) indicate that this decrease can reach up to 1 PW in the total EHF at tropical regions.

[11] The effect of the wind in the determination of the annual mean EHF is not as conspicuous. There are characteristics of the wind measurement that are inherent to the instruments. ERS winds tend to have a low bias when compared to buoy measurements [*Quilfen et al.*, 2001]. This bias varies seasonally and geographically. ERS winds also tend to be lower than those measured by SSMI [*Boutin et al.*, 1999]. They compared SSMI winds with ERS and NSCAT winds and found that the spatial variability of the difference between ERS and NSCAT is substantially less than that between SSMI and NSCAT.

[12] The estimation of the wind stress from the wind speed is generally done through the use of a bulk aerodynamical formulation. However, when the boundary layer stability is taken into account, as in *Liu et al.* [1979], the results gain accuracy, particularly in regions where the air-sea temperature difference is significant.

[13] The ERS wind data set has its limitations as do other data sources. The reasons that explain the discrepancies between ERS and other wind sources remain mostly unsolved. Although a comprehensive discussion of these differences would improve our conclusions, it is clearly out of scope of this study. Nevertheless, the long duration and the continuity of the mission in addition to the consistency with the NSCAT winds outweigh the problems due to the bias since we are looking for inter-annual trends.

[14] The intra-decadal variability in the EHF is obtained by the subtraction of a sinusoidal annual cycle from the time series. To show the robustness of the intra-decadal signal, the EHF residuals (EHF′) are averaged for several latitudi-

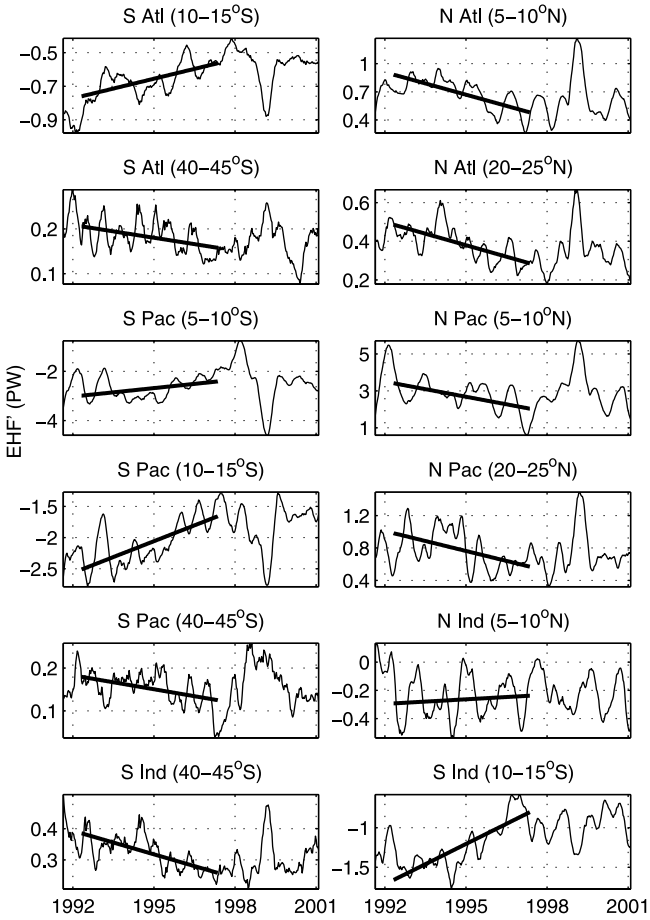

Figure 2. EHF′ time series averaged at various latitudinal bands (in parentheses) in the Atlantic, Pacific, and Indian ocean basins. The straight lines represent the linear fit for the period between May, 1992 and May, 1997.

nal bands, Figure 2. These bands show the long-term trend variations in the three basins and how its intensity changes with latitude. There is a clear decrease in the magnitude of the annual mean of the EHF′ between the 1992–1994 and 1995–1997 periods in the tropical regions of the Atlantic and Pacific. There is also a slight decrease in the equatorward EHF′ at higher latitudes. In the Pacific, the El Niño of 1998 seems to stop the inter-annual changes restoring the EHF′ annual mean back to the levels observed in 1992. These pentadal changes are significant and depending on the latitude they surpass the amplitude of the annual cycle.

[15] A linear regression was performed for the period between May, 1992 and May, 1997 to estimate the long-term change in EHF′. Prior to this period the ERS1 was still in the adjustment phase. The linear model is: $Q_{fit} = a.t + b$, where a is the slope of the fit, t is the time in years, and b is the bias. The coefficient a measures the trend of the EHF′ for the 5-year period in question. Figure 3 shows the changes in the EHF′ for the 5-year period as the end points difference of the estimates obtained by the linear fit.

[16] In general, the poleward flux of warmer waters in the Ekman layer decreases in the tropical Pacific and Atlantic oceans. In the tropical northern hemisphere the annual mean of the northward EHF′ decreases along the pentad. Similarly, in the southern hemisphere the poleward flux, which is southward, also decreases in magnitude during the same period. Moreover, the EHF′ is approximately anti-symmetric with respect to the Equator in the Atlantic. However, the trends in the Pacific are not similar in both hemispheres: there is an abrupt change in the slope of the pentadal trend around 13.5°S. In the North Pacific, the pentadal changes reach −1.5 PW in the northern hemisphere while in the South Pacific the changes are at most 0.9 PW at 13.5°S. In the South Indian Ocean the southward flow also has a decreasing trend with a maximum of 1.0 PW at 9.5°S. In the North Indian ocean the changes are not significant. This is probably because the basin is relatively small and closed to the north. Overall, the sum of all contributions show that the global poleward flow decreased in the tropics between 1992 and 1997.

[17] Changes in the EHF′ are caused by changes in the wind stress or in the temperature field. To test which of these factors is predominant we compared the EHF estimated by either suppressing the variability in the Ekman temperature field ($E_1' = -c_p \int_0^L \tau_x(\theta_e - \overline{\theta})/f dx$) or in the wind stress ($E_2' = -c_p \int_0^L \overline{\tau_x}(\theta_e - \overline{\theta})/f dx$). The over bar quantities represent temporal averages. These Ekman heat fluxes are estimated as a function of latitude, the annual cycle is removed, and the 5-year linear trend is estimated as before. The changes in the total global EHF′ as a function of temperature (E_2') are significantly smaller compared to when we allow for wind stress fluctuations (E_1'). This result is not shown here, but EHF′ is very similar to E_1' mostly everywhere while E_2' is almost zero. Therefore, these tests show that changes in the EHF are dominated by changes in the wind field.

[18] It is important to notice that the pentadal changes in the EHF are significant when compared to other relevant variability components. For instance, several direct estimates using hydrographic sections in all basins associate an error of about 0.3 PW to the determination of the total meridional heat flux [*Macdonald and Wunsch*, 1996]. From Figure 3 it is evident that the intra-decadal changes can be larger than that, specially for low latitudes.

[19] The question that still remains is the consistency of the EHF trends using different wind products. We have

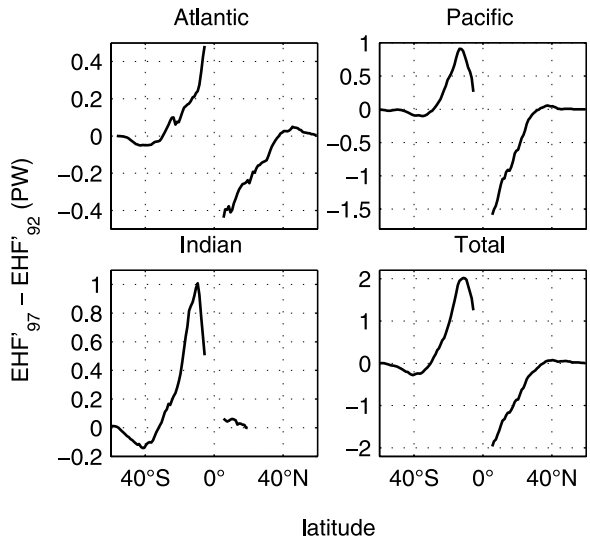

Figure 3. Change in the EHF′ for the Atlantic, Pacific, Indian, and the total for the period between 1992 and 1997.

compared our results with the EHF obtained from the directional SSMI winds [*Atlas et al.*, 1996]. The results based on SSMI (not presented) show a somewhat similar trend in the North Atlantic. Near the Equator the long-term trend in the EHF′ is about −0.4 PW, as observed for the ERS data. The EHF′ as a function of latitude is similar between the two data sets in the South Indian Ocean. For the other basins the trend as a function of latitude does not agree between ERS and SSMI. The cause for the discrepancies in the results drawn from these two satellite wind products are not further pursued. A detailed inter-comparison of these wind products is beyond the scope of this study.

[20] The SSMI wind data do not corroborate the long-term trend in a global scale. However, our results from ERS1/2 data come to complement a recent study done by *McPhaden and Zhang* [2002]. They showed inter-decadal trends in the Ekman heat transport in the Pacific Ocean related to a relaxation of the trade winds between the 1970s and 1990s. They have used four wind data products for their analysis, none of them from satellite sources. Therefore, our results based on satellite observations are not only consistent with theirs but extend the picture of the slowing down of the meridional circulation to a global scale.

4. Conclusions

[21] The intra-decadal changes in the EHF could have a profound impact in climate variability. The present study shows evidence that the wind-driven circulation promoted in the Ekman layer was sending less warm waters to the poles from 1992 to 1997 and that this trend was only restored by the start of a very strong El Niño event. Because of the time series limitations we could not make more inferences about other El Niño events, yet the presented evidences show the global reach of the EHF changes tied to the El Niño mechanism.

[22] Although the agreement between the EHF estimates from SSMI and ERS is not verified for all basins, the ERS-based estimates corroborate the results from *McPhaden and Zhang* [2002]. They have averaged four different sources of wind, none of which was satellite derived. Thus, our study can be considered an independent validation. The effect of the ERS low-biased winds is an overall decrease of the EHF. Because the many validation studies presented no evidence until now that this bias has any form of long-term variability, it seems reasonable to assume that the intra-decadal changes are of geophysical origin.

[23] We stressed here the importance of the ocean heat flux in the climate system and examined the temporal variability observed in the EHF component. The accurate determination and monitoring of the EHF trend was possible because of the long and continuous ERS scatterometer missions. We showed that the evidences for inter-annual changes in a scale of five years in the EHF are striking in a global scale. However, the EHF is only one piece of the puzzle. To determine if the trends really affect the total oceanic heat flux we still have to know the geostrophic component, that is, the contributions from the vertical overturning and the gyre circulation. If these pentadal changes in the EHF are not compensated by their geostrophic counterparts they could have an impact in the deep water formation. Due to the long time scale of this oceanic response it could cause measurable changes in the global climate on a decadal time scale.

[24] **Acknowledgments.** This study was partly performed at the Jet Propulsion Laboratory, California Institute of Technology supported by the Physical Oceanography and Earth Observing System Interdisciplinary Sciences Programs of NASA. Final stages of this study were performed and supported by the Instituto Nacional de Pesquisas Espaciais (INPE) Brazil. We thank the reviewers for their comments and suggestions.

References

Adamec, D., M. M. Rienecker, and J. M. Vukovich, The time-varying characteristics of the meridional Ekman heat transport for the world ocean, *J. Phys. Oceanogr.*, *23*, 2704–2716, 1993.

Atlas, R., R. Hoffman, S. Bloom, J. Jusem, and J. Ardizzone, A multi-year global surface wind velocity data set using SSM/I wind observations, *Bull. Amer. Meteor. Soc.*, *77*(5), 869–882, 1996.

Böning, C. W., and P. Herrmann, Annual cycle of poleward heat transport in the ocean: Results from high resolution modeling of the North and Equatorial Atlantic, *J. Phys. Oceanogr.*, *24*, 91–107, 1994.

Boutin, J., J. Etcheto, M. Rafizadeh, and D. C. E. Bakker, Comparison of NSCAT, ERS 2 active microwave instrument, Special Sensor Microwave Imager, and Carbon Interface Ocean Atmosphere buoy wind speed: consequences for the air-sea CO_2 exchange coefficient, *J. Geophys. Res.*, *104*, 11,375–11,392, 1999.

Bryden, H. L., and M. M. Hall, Heat transport by currents across 25°N latitude in the North Atlantic, *Science*, *207*, 884–885, 1980.

Bryden, H. L., D. H. Roemmich, and J. A. Church, Ocean heat transport across 24°N in the Pacific, *Deep-Sea Res.*, *40*, 297–324, 1991.

Dong, B.-W., and R. T. Sutton, The dominant mechanisms of variability in Atlantic ocean heat transport in a coupled ocean-atmosphere GCM, *Geophys. Res. Let.*, *28*, 2445–2448, 2001.

Ghirardelli, J. E., M. M. Rienecker, and D. Adamec, Meridional Ekman heat transport: Estimates from satellite data, *J. Phys. Oceanogr.*, *25*, 2741–2755, 1995.

Hall, M. M., and H. L. Bryden, Direct estimates and mechanisms of ocean heat transport, *Deep-Sea Res.*, *29*, 339–359, 1982.

Kraus, E. B., and S. Levitus, Annual heat flux variations across the tropic circles, *J. Phys. Oceanogr.*, *16*, 1479–1486, 1986.

Levitus, S., Meridional Ekman heat fluxes for the world ocean and individual ocean basins, *J. Phys. Oceanogr.*, *17*, 1484–1492, 1987.

Levitus, S., and T. P. Boyer, World Ocean Atlas 1994, *Tech. Rep.* Vol. 4: *Temperature*, National Oceanographic Data Center, Ocean Climate Laboratory, 129 pp, 1994.

Liu, W. T., K. B. Katsaros, and J. A. Businger, Bulk paramerizations of air-sea exchanges of heat and water vapor including molecular constraints at the interface, *J. Atmos. Sci.*, *36*, 1722–1735, 1979.

Macdonald, A. M., and C. Wunsch, A global estimate of the ocean circulation and heat fluxes, *Nature*, *382*, 436–439, 1996.

McPhaden, M. J., and D. Zhang, Slowdown of the meridional overturning circulation in the upper Pacific Ocean, *Nature*, *415*, 603–608, 2002.

Montgomery, R. B., Comments on "Seasonal variability of the Florida current," by Niiler and Richardson, *J. Mar. Res.*, *32*, 533–535, 1974.

Polito, P. S., O. Sato, and W. T. Liu, Characterization of the heat storage variability from TOPEX/POSEIDON at four oceanographic sites, *J. Geophys. Res.*, *105*(C7), 16,911–16,921, 2000.

Quilfen, Y., B. Chapron, and D. Vandemark, On the ERS scatterometer wind measurement accuracy: Evidence of seasonal and regional biases, *J. Atmos. Oceanic Technol.*, *18*, 1684–1697, 2001.

Rago, T. A., and H. T. Rossby, Heat transport into the North Atlantic Ocean north of 32°N latitude, *J. Phys. Oceanogr.*, *17*, 854–871, 1987.

Reynolds, R. W., and T. M. Smith, Improved global sea surface temperature analysis using optimal interpolation, *J. Climate*, *7*, 929–948, 1994.

Sato, O. T., and T. Rossby, Seasonal and low frequency variability in the meridional heat flux at 36°N in the North Atlantic, *J. Phys. Oceanogr.*, *30*(3), 606–621, 2000.

O. T. Sato and P. S. Polito, Instituto Nacional de Pesquisas Espaciais (INPE), Divisão de Sensoriamento Remoto (SERE II), Ave. dos Astronautas, 1758, São José dos Campos, SP 12227-010, Brazil. (olga@ltid.inpe.br)

W. Timothy Liu, Jet Propulsion Laboratory/Caltech, Pasadena, CA, USA.